ChinaRxiv

AI translation · View original & related papers at
chinarxiv.org/items/chinaxiv-201701.00233

A Novel Ground-Based Fabry-Perot Interferometer for Measuring Thermospheric Winds Postprint

Authors: Wang Houmao, Wang Yongmei, Fu Jianguo, Zhang Zhongmou

Date: 2017-01-22T00:00:00+00:00

Abstract

Owing to the extreme thinness of the atmosphere at an altitude of ~250 km above Earth, passive optical observation is currently the most effective means for detecting wind fields in this layer. The Fabry-Perot interferometer (FPI), featuring high energy utilization efficiency and spectral resolution, is one of the most effective ground-based instruments for wind field detection in this atmospheric layer. To date, FPI has been employed for upper atmospheric wind field detection for several decades, with many countries utilizing various FPIs to observe the 630.0 nm nightglow and thereby retrieve upper atmospheric wind fields. The Center for Space Science and Applied Research, Chinese Academy of Sciences (CAS) has developed a compact FPI with relatively low cost by employing a beam reduction system and post-filter (after the etalon) configuration. The instrument primarily comprises a telescope scanning system, an etalon system, a beam reduction and filter system, a detector system, and a laser calibration system, with an overall size of 1.34$×0.58×$0.35 m3, making it suitable for field ground-based or vehicle-mounted wind field measurements. Based on this compact FPI, ground-based observation experiments were conducted in 2014 at Langfang, Hebei (39.40°N, 116.65°E) and Kelan, Shanxi (38.71°N, 111.58°E), where observation data were combined with retrieval algorithms to obtain upper atmospheric wind field data, and the results were intercompared with wind field data from two FPIs at the National Center for Atmospheric Research (NCAR), yielding an average retrieval deviation of 11.8 m/s (Kelan).

ChinaRxiv 中X

Full Text

A Novel Ground-Based Fabry-Perot Interferometer for Thermospheric Wind Measurements

WANG Houmao*, WANG Yongmei, FU Jianguo, ZHANG Zhongmou
Center for Space Science and Applied Research, Chinese Academy of Sciences, Beijing 100190

Abstract

Passive optical observation is currently the most effective method for wind field detection in the upper atmosphere at altitudes of approximately 250 km due to the extreme thinness of the air at these heights. The Fabry-Perot interferometer (FPI) offers high energy utilization and spectral resolution, making it one of the most effective ground-based instruments for probing winds in this atmospheric layer. For decades, FPIs have been employed for upper atmospheric wind field measurements worldwide, with numerous countries using various FPI configurations to observe the 630.0 nm nightglow emission and retrieve thermospheric wind velocities. The National Space Science Center of the Chinese Academy of Sciences has developed a compact, relatively low-cost FPI employing a beam reduction system and a post-etalon filter configuration. The instrument comprises five main subsystems: a telescope scanning system, an etalon system, a beam reduction and filter system, a detector system, and a laser calibration system. With overall dimensions of $1.34\$\times0.58\times0.35m\^{}\{3\}\$$, the instrument is well-suited for portable ground-based or vehicle-mounted wind measurements. Using this miniaturized FPI, ground-based observation experiments were conducted in 2014 at Langfang, Hebei (39.40°N, 116.65°E) and Kelan, Shanxi (38.71°N, 111.58°E). The observational data were combined with retrieval algorithms to obtain upper atmospheric wind field measurements, which were then compared with data from two FPI instruments operated by the U.S. National Center for Atmospheric Research. The average retrieval deviation was 11.8 m/s at the Kelan site.

Keywords: Fabry-Perot interferometer (FPI), upper atmospheric wind field, ground-based observation, 630.0 nm nightglow

1 Introduction

The wind field in the middle and upper atmosphere represents one of the fundamental parameters of this region, playing a crucial role in energy transport within the middle and upper atmosphere as well as between atmospheric layers. It also significantly impacts the safety and orbital operations of spacecraft, making it an essential space environment parameter. Consequently, wind measurements serve as important foundational data for atmospheric model development and provide critical observational data for studying coupled atmospheric dynamics and photochemical processes. Among passive optical instruments cur-

rently used for wind measurements, the primary options include Fabry-Perot interferometers, Michelson interferometers, and asymmetric spatial heterodyne interferometers. The FPI offers several advantages, including high sensitivity, high spectral resolution, and a simple structure with no moving parts in its optical path. As a static interferometric imaging spectroscopy technique, it demonstrates high stability, strong resistance to vibration interference, and high energy utilization and detection sensitivity, leading to its widespread application in both ground-based and spaceborne measurements of middle and upper atmospheric winds [1].

Internationally, research on middle and upper atmospheric wind field detection using FPIs began in the 1980s. In 1982, the Fabry-Perot interferometer aboard the DE-2 satellite (DE-FPI) achieved the first spaceborne measurement of upper atmospheric winds. In September 1991, the FPI instrument on the UARS satellite was successfully launched, enabling measurements of wind velocity, temperature, and volume emission rate in the mesosphere and lower thermosphere with a measurement error of 5 m/s [2-4]. In 2001, the TIDI Doppler imager aboard the TIMED satellite employed a single FPI etalon to achieve rapid all-weather observations of winds in the middle and upper atmosphere while simultaneously measuring atmospheric temperature and trace constituents, with retrieval errors reaching 3 m/s [5-7].

Relative to spaceborne detection, ground-based wind observations began even earlier internationally, with initial efforts dating to the 1960s [8-9]. Numerous countries and research groups have developed various FPI configurations for measuring middle and upper atmospheric winds. Between 1969 and 1985, the NOAA Aeronomy Laboratory installed two Fabry-Perot spectrometers at the Fritz Peak Observatory in Colorado for wind measurements [10]. Subsequently, the University of Michigan and the NCAR High Altitude Observatory, among others, conducted ground-based wind measurements using FPIs, achieving errors of 6 m/s [11-12]. Since the late 1980s, Japan has employed ground-based FPIs to observe both OI 630.0 nm and OI 557.7 nm airglow emissions, with measurement accuracies of 10-50 m/s and 2-13 m/s, respectively [13-14]. In recent years, the United States has attempted daytime ground-based observations using FPIs and obtained preliminary results [15-16]. Following these developments, FPI instruments have gradually evolved toward miniaturization to reduce manufacturing costs, with both the United States and Japan adopting smaller-aperture etalons for wind measurements [17-18].

In China, ground-based wind measurements have only begun in recent years [19]. In 2010, the National Space Science Center imported an FPI from the U.S. National Center for Atmospheric Research, achieving China' s first middle and upper atmospheric wind observations using an optical interferometer [20-21]. Regarding instrument development, research has primarily been conducted by the National Space Science Center of the Chinese Academy of Sciences and Wuhan University. This paper presents upper atmospheric wind measurements obtained using the miniaturized FPI developed by the National Space Science

Center and compares these measurements with results from the U.S. National Center for Atmospheric Research' s FPI instruments.

2.1 Instrument Design

The FPI optical system consists of four main components (Figure 1 [FIGURE:1]): a sky scanning system, an etalon system, a beam reduction and filter system, and a detector system. (1) The sky scanning system comprises two 45° parallel plane mirrors, each with a diameter of 10 cm, providing a total field of view of 2.25°. One mirror can rotate in the horizontal direction while the other can rotate vertically, allowing combined observation of any azimuth and zenith angle in the sky. (2) The etalon has an aperture of 13 cm and a spacing of 1.5 cm, with a reflectivity of 0.76. The entire etalon system is temperature-controlled at 30$\pm$0.1°$Ctosuppressinterferenceringdriftcausedbytemperaturevariations.(3)Thebeamreductionsystemisp$ making it highly portable and suitable for vehicle-mounted measurements.

For ground-based observations, measurements are sequentially taken in five directions: zenith, east, west, south, and north. The zenith angle is 90° for the zenith direction and 45° for all other directions. Due to the relatively weak 630.0 nm airglow emission, the integration time for each direction is relatively long at 5 minutes, resulting in a sampling interval of approximately 30 minutes for each complete dataset (all five directions).

2.2 Data Processing

Since the wind velocity obtained from Doppler shift represents the line-of-sight wind, one method for deriving horizontal wind speeds involves measurements from opposite directions at the same zenith angle. Specifically, north-south observations can be used to retrieve meridional winds, while east-west observations yield zonal winds [13]. In the calculation method, V_N represents zonal wind speed (positive northward), V_E represents meridional wind speed (positive eastward), is the observation zenith angle, c is the speed of light, r is the interference ring radius, and the subscripts E, W, S, and N denote east, west, south, and north directions, respectively. The data processing workflow proceeds as follows [22,23]:

(1) Preliminary estimation of the interference ring center coordinates (C_x, C_y).

(2) Based on laser calibration data, accurate determination of the interference ring center using an iterative method combined with Gaussian fitting, with the initial center coordinates as the starting point.

(3) Performing circular integration centered on the determined center to transform the two-dimensional interference rings into a one-dimensional interference curve.

(4) Since the intensity near the interference fringe peaks follows a Gaussian distribution, using a Gaussian fitting function to determine each interference fringe peak and thereby obtain the interference ring radius.

(5) Calculating the meridional and zonal wind speeds using Equation (1) and Equation (2), respectively.

3 Experimental Results and Comparative Analysis

Currently, ground-based FPI instruments have been deployed at Xinglong (40.40°N, 117.59°E) and Kelan, both developed by the U.S. National Center for Atmospheric Research (NCAR). We therefore designate their wind results as A-NCAR. For our study, we selected Langfang and Kelan for observation experiments. The specific locations of the three stations are shown in Figure 2

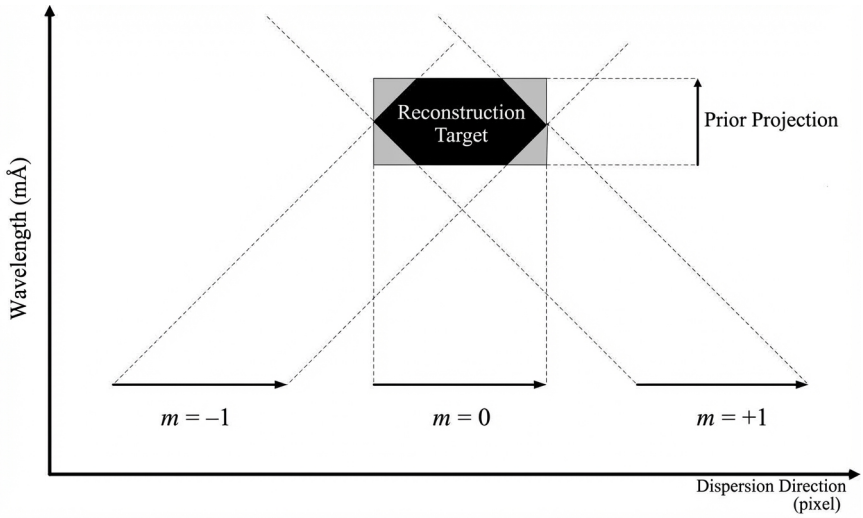

Figure 1: Figure 2

. Since all three sites are located in mid-latitude regions with inter-site distances of $ $500 km, we can perform approximate inter-comparison and analysis using observational data from the three stations.

The observation experiments consisted of two main campaigns. The first was conducted in Langfang from September 24-25, 2014. Due to weather conditions, we obtained wind data only for September 24, which we compared with observations from the two NCAR FPI instruments at Xinglong and Kelan (Figure 3 [FIGURE:3]). The wind velocity variations from the three FPI instruments show consistent trends, with relatively larger differences occurring around midnight due to weakening airglow emissions and increased random errors in wind retrieval. For example, the maximum errors occurred at approximately 16:30

UTC (local time: 00:30 the following day), reaching 14 m/s (Langfang), 34 m/s (Kelan), and 18 m/s (Xinglong), with correspondingly larger differences in wind results among the three stations.

The second experiment was conducted in Kelan from October 16-26, 2014. Due to weather and ambient temperature control issues, we obtained approximately five days of data (Figure 4 [FIGURE:4]). Comparative analysis reveals an average wind speed deviation of 11.8 m/s over the five-day period. This demonstrates relatively good agreement between the two instruments, indicating that our FPI can be effectively applied to atmospheric wind field measurements.

This paper presents ground-based measurements of upper atmospheric wind fields using a miniaturized FPI employing a post-etalon beam reduction system and filter configuration. The developed FPI includes a telescope scanning system, etalon system, beam reduction and filter system, detector system, and laser calibration system, with dimensions of 1.34$×0.58×0.35$m^{3}$, making it suitable for mobile ground-based and vehicle-mounted wind measurements. Using this instrument, we conducted ground-based observation experiments in Langfang, Hebei, and compared our retrieval results with those from two U.S. A-NCAR instruments (at Xinglong and Kelan). Subsequently, we performed additional observation experiments in Kelan, Shanxi, and compared these results with the Kelan A-NCAR FPI wind data, obtaining an average retrieval deviation of 11.8 m/s. These results demonstrate that our FPI instrument can be effectively used for ground-based detection of atmospheric wind fields.

Acknowledgments

We thank the National Space Science Center of the Chinese Academy of Sciences and the National Satellite Meteorological Center of the China Meteorological Administration for providing the ground-based FPI observation data and wind products.

References

[1] Han Weihua, Wang Yongmei, Lü Jiangong, et al. Auto-processing of Middle and Upper Atmosphere Wind FPI Interference Fringe Pattern. Science Technology and Engineering, 2010, vol.10, No.10. In Chinese
[2] W R Skinner, P B Hays, V J Abreu. High resolution Doppler imager [C]. Ann Arbor: International Geoscience and Remote sensing Symposium, 1987: 673~676.
[3] V J Abreu, P B Hays, W R Skinner. The high resolution Doppler imager [J]. Opt. Photon. News, 1991, 2(10): 28~30
[4] P B Hays, B J Abreu, M E Dobbs, et al. The High-Resolution Doppler Imager on the Upper Atmosphere Research Satellite. Journal of Geophysical Research, 1993, vol.98, no. D6, 10713~10723
[5] T L Killen, W R Skinnerm, R M Johnson, et al. TIMED Doppler interferometer (TIDI) [C]. SPIE, 1999, 3756: 289~301

[6] W R Skinner, R J Niciejewski, T L Killen, et al. Operational performance of the TIMED Doppler interferometer (TIDI) [C]. SPIE, 2003, 5157: 47~57
[7] T L Killeen, Q Wu, S C Solomon, et al. TIMED Doppler Interferometer: Overview and recent results. J. Geophys. Res., 111, A10S01, doi: 10.1029/2005JA011484, 2006
[8] T L Killen, B C Kennedy, P B Hays, et al. Image plane detector for the dynamics explorer Fabry-Perot interferometer [J]. Appl. Opt., 1983, 22(22): 3503~3513
[9] T L Killeen, P B Hays. Doppler line profile analysis for a multichannel Fabry-Perot interferometer [J]. Appl. Opt., 1984, 23(4): 612~620
[10] G. Hernandez, R. G. Roble, E. C. Ridley, J. H. Allen. Thermospheric response observed over Fritz Peak, Colorado, during two large geomagnetic storms near Solar Cycle Maximum. Journal of Geophysical Research. Volume 87, Issue A11, pages 9181-9192, 1982
[11] Rick Niciejewski, Timothy L. Killeen, Matthew Turnbull. Ground-based Fabry-Perot interferometry of the terrestrial night glow with a bare charge-coupled device: remote field site deployment. Optical Engineering. Vol. 33, No. 2, 457~465, 1994
[12] Qian Wu, R D Gablehouse, S C Solomon, et al. A New Fabry-Perot Interferometer for Upper Atmosphere Research. Proc. of SPIE. Vol. 5660, 218~227. Doi: 10.1117/12.573084, 2004
[13] K Shiokawa, T Kadota, M K Ejiri, et al. Three-channel imaging Fabry-Perot interferometer for measurement of mid-latitude airglow. Applied Optics. Vol. 40, N0. 24, 4286~4296, 2001
[14] K Shiokawa, T Kadota, Y Otsuka, et al. A two-channel Fabry-Perot interferometer with thermoelectric-cooled CCD detectors for neutral wind measurement in the upper atmosphere. Earth Planets Space, 55, 271~275, 2003
[15] Gerrard A. J. and J. W. Meriwethe. Initial daytime and nighttime SOFDI observations of thermospheric winds from Fabry-Perot Doppler shift measurements of the 630-nm OI line-shape profile. Ann. Geophys. 29, 1529-1536, 2011
[16] Wu Q., W. Wang, R. G. Roble, et al. First daytime thermospheric wind observation from a balloon-borne Fabry-Perot interferometer over Kiruna (68N). GEOPHYSICAL RESEARCH LETTERS. 39, L14104, Doi:10.1029/2012GL052533, 2012
[17] Makela J J, John W. Meriwether, Yiyi Huang, and Peter J. Sherwood. Simulation and analysis of a multi-order imaging Fabry–Perot interferometer for the study of thermospheric winds and temperatures. APPLIED OPTICS, Vol. 50, No. 22, 4403-4416, 2011
[18] Shiokawwa K., Otsuka Y., Oyama S., et al. Development of low-cost sky-scanning Fabry-Perot interferometer for airglow and auroral stydies. Earth Planets Space, vol.64, no.11, 1033-1046, 2012
[19] Wang H M, Wang Y M, Wang Y J. Data processing of the middle and upper atmospheric wind retrieval based on the Fabry-Perot Interferometer. Chinese J. Geophys., 2013, 56(4): 1095-1101, doi: 10.6038/cjg20130405. In Chinese

[20] Yuan Wei, Xu Jiyao, Ma Ruiping, et al. First observation of mesospheric and thermospheric winds by a Fabry-Perot interferometer in China, Chinese Science Bulletin, 2010, 55,(35), 4046-4051. In Chinese
[21] Jiang G Y, Xu J Y, Yuan W, et al. A comparison of mesospheric winds measured by FPI and meteor radar located at 40N. Sci China Tech Sci, 2012, 55: doi: 10.1007/s11431-012-4773-1
[22] Wang Houmao, Wang Yongmei, Wang Yingjian, et al. Wind retrieval and error analysis of the ground-based Fabry-Perot Interferometer for the middle and upper atmosphere. Chin. J. Space Sci., 2014, 34(4):415-425. In Chinese
[23] Wang H., Wang Y. Error calculation and analysis for an improved wind retrieval method based on the ground-based Fabry-Perot interferometer measurements, Advances in Space Research (2015), doi: http://dx.doi.org/10.1016/j.asr.2015.03.010

Author Information:
Email: hmwang@nssc.ac.cn
Contact: 010-62582629, 13810639527

Source: ChinaXiv —Machine translation. Verify with original.